

Mathematical Model for Segmentation of Medical Images via Hybrid Images Data

Hadia Atta
Department of Mathematics,
Islamia College Peshawar, Pakistan,
Email: hadiaatta@gmail.com

Noor Badshah
Department of Basic Sciences,
University of Engineering and Technology, Peshawar, Pakistan,
Email: noor2knoor@gmail.com

Syed Inayat Ali Shah
Department of Mathematics,
Islamia College Peshawar, Pakistan,
Email: inayat64@gmail.com

Nasru Minallah
Department of Computer Systems Engineering,
University of Engineering and Technology, Peshawar, Pakistan,
Email: minallah.nasru@gmail.com

Abstract. The analysis of medical images requires image segmentation to distinguish the boundaries of irregular regions such as tumors in images. However, segmentation of medical images with intensity inhomogeneity has always been a challenging task in image processing. In this paper, we have proposed a new model for segmentation of medical image having inhomogeneous intensities. In the proposed model, we have used hybrid image data obtained from the product of given image with smooth image and difference of smooth product image from product image. The model uses both local and global information of the image. The proposed model outperforms the existing models qualitatively and quantitatively i.e. in terms of number of iterations and CPU time. For the solution of proposed model we have used some of the numerical schemes such as Explicit and Semi-Implicit schemes. The model is further tested for different type of real medical images. The results showed that the proposed model also performs well in images having intensity inhomogeneity and blurred edges as well.

AMS (MOS) Subject Classification Codes: 35S29; 40S70; 25U09

Key Words: Intensity inhomogeneity, Segmentation, Level set, Region of interest.

1. INTRODUCTION

Segmentation of images having intensity inhomogeneity is a demanding and challenging task nowadays. Inhomogeneity in images exists due to the spatial modification in brightness and smooth intensity variability, which may be influenced by radio frequency penetration, gradient driven eddy currents, inhomogeneous reception sensitivity profile etc [8]. The purpose of the segmentation is to divide an image into meaningful sub-domains under some specific criterion. The region in an image with intensity inhomogeneity to be segmented is due to the overlap between the ranges of the intensities. Based on different pixel intensities in a required region, this becomes more challenging to recognize the objects of interest [9]. In such cases, poor segmentation may be observed in "intensity-based" segmentation methods [8]. This misclassification is produced on account of extended deviations of intensity distributions of each object so that it is challenging to detect objects completely based on their specific intensity distributions [18].

For image segmentation, two fundamental variational models are snake model [7] proposed by Kass et al. and Mumford Shah (MS) model [12] proposed by Mumford et al. The snake model [7] is a typical parametric active contour model (ACM) based on image edges for fast segmentation. However, this model is not efficient and effective for the images having weak boundaries and for adaptive topologies. The MS model (region based model) [12], aims to find the contour by segmenting an original image into non-overlapping regions and a piecewise smooth image as an approximation of the original image. The main limitation of the MS model is that the energy function is difficult to minimize because the function of this model is non-convex and also has unknown contour [4, 17].

Region based models are widely used in the image segmentation process. Region based models assume homogenous image intensities in the region of interest. That is the way it frequently fails to provide precise results of segmentation in images having inhomogeneous intensity [8]. In region based methods, the intensities in the region to be segmented usually depend on a region descriptor/statistics i.e. variance or coefficient of variation. However, it is difficult to obtain such a region descriptor in images having inhomogeneous intensity, which makes the segmentation process complicated on the basis of pixel intensities [2]. For image segmentation, Chan and Vese presented a region based active model model named CV model [3], under the assumptions that in each region, the image has a different mean pixel intensity and also image comprises of two statistically homogeneous regions [10]. The CV model [3] is suitable for images having piecewise constant functions but this model is not appropriate for images with intensity inhomogeneity [18, 5]. To overcome the problem of intensity inhomogeneity, Li et al. [11] presented LBF model "Local binary fitting model". By introducing a kernel function in local binary fitting energy and using the information of local region [6], the LBF model can efficiently segment the images with inhomogeneous intensity [11] and weak boundaries [19]. But this model usually relies on the initial placement of contour [13].

In the existence of inhomogeneous intensity and noise, models based on local mean intensity in image segmentation are not capable of providing precise segmented results. To overcome the limitation of intensity inhomogeneity in images, Wang et al. [14], therefore presented an improved model named "Local Gaussian Distribution Fitting" (LGDF) Energy model. For more precise segmentation this model utilizes more local information in terms of a Gaussian distribution with different variances and means. In local intensities the variances and means are regarded as spatially varying functions to recognize the variations among the background and foreground regions. The LGDF model has the ability of manipulating images having inhomogeneous intensity and noises [15]. Though the LGDF model, to some extent is sensitive to initialization [16], it merely uses only information of local intensity which may fail to acquire the required objects entirely from an image [15]. Hence, the LGDF restricts their practical applications. The LGDF model may not give accurate segmentation results as shown in experimental results and may have a slow convergence rate. To deal the images with inhomogeneous intensity, Haider et al. [1] presented a new region based variational model named as Double Fitting Terms of Multiplicative and Difference Images (DMD) model. This model consists of the combination of multiplicative and difference of an images considered as two fitting terms based on regions and edges improved quantities. The DMD model is not sensitive to initial contours and can process images having noise and inhomogeneous regions [1]. The main limitation of the DMD model is that it does not only detect the infected area but also detects all the regions in an image especially in medical images. The above traditional region based models [3, 14, 1], which were presented in the context of binary images, in some extent do not perform well in the existence of inhomogeneous intensity regions in the target image.

Our main focus is to overcome the limitations of the LGDF and the DMD models. In this paper, we have focused on a new novel region based model for segmentation of different medical images having inhomogeneous intensities. This paper presents a new model i.e. local Gaussian Distribution Fitting Energy model which uses the information of both multiplicative and difference of an image. The global and local informations are described by multiplication and difference of an image, respectively. Our proposed model can be used for precise segmentation in images having severe intensity inhomogeneity and with blurred edges. For the solution of proposed model we implemented numerical schemes such as Explicit and Semi Implicit Schemes. And compared results of proposed model with other existing models in terms of qualitatively through number of iterations and computational (CPU) time and quantitatively through Jaccard Similarity Index (JSI).

The remaining part of a paper is designed in the following way. In section 2, we have reviewed some background material with their limitations. The proposed model is presented in section 3 with implementation of an algorithm. Section 4 consists of numerical schemes. Experimental results and discussions are presented and discussed in section 5. Conclusions are given in section 6.

2. BACKGROUND MATERIALS

In this section we have discussed some of the existing models for motivation towards the development of a novel model.

2.1. Active Contours Without Edges (CV) Model. Chan et al. in [3] presented a region based model for images having homogeneous intensities. This model is the special case of piecewise constant Mumford Shah model [12], by dividing a given image into two regions, namely foreground and background. The energy functional of the model is given as:

$$F_{CV}(a_1, a_2, S) = \lambda_1 \int_{in(S)} |I - a_1|^2 dx + \lambda_2 \int_{out(S)} |I - a_2|^2 dx \quad (2. 1) \\ + \mu Length(S),$$

where a_1, a_2 are the average intensities of a given image I inside and outside of a variable contour S respectively, $\lambda_1, \lambda_2, \mu$ are the nonnegative parameters. The first two terms in equation (2. 1) give an approximation of the given image by constants in two different regions, while the third term is responsible for smoothness/regularization. In this model, level sets were used for the first time in region based segmentation models. The model is then minimized using the Euler Lagrange's equation to get a nonlinear partial differential equation, which is then solved by applying the Semi Implicit method. This model works well in such images which have homogeneous regions and also obtain satisfactory results in noisy images without filtering. It also detects objects in an image whose boundaries are not well defined by the gradient [10, 19].

Since the CV model is a non-convex so there are more chances that it may stuck at local minima. This model does not show good results in segmenting images having inhomogeneity because of considering constant values in each region [5]. One step towards handling inhomogeneous images is taken by Wang et al in [14], which is discussed in the next section briefly.

2.2. The Local Gaussian Distribution Fitting (LGDF) Based Active Contour Model.

Wang et al. in [14] proposed a region based model for segmentation of images having inhomogeneous intensity. In this model the local image intensities are described by a Gaussian distribution with variables such as means and variances. This model uses the information of the local intensity through the partition of neighborhood described in a circular window [15]. The proposed local fitting energy functional in terms of level set ψ is as follows:

$$F_{LGDF} = \nu L(\psi) + \mu P(\psi) - \int \omega_\sigma(x - y) \log p_{\{1,x\}}(I_0(y)) \Upsilon_1(\psi(y)) dy dx \\ - \int \omega_\sigma(x - y) \log p_{\{2,x\}}(I_0(y)) \Upsilon_2(\psi(y)) dy dx, \quad (2. 2)$$

where $\omega_\sigma(x - y)$ is a local circular window center at x , $\Upsilon_j(\psi(x))$ for $j = 1, 2$ are the characteristic functions (region descriptors). $p_{(j,x)}$ for $j = 1, 2$ are the probability density functions and are defined by:

$$p_{\{j,x\}} = \frac{1}{\sqrt{2\pi}\sigma_j(x)} \exp\left(\frac{-(u_j(x) - I_0(y))^2}{2\sigma_j(x)^2}\right),$$

where $u_j(x)$ and $\sigma_j(x)$ for $j = 1, 2$ are the intensity means and standard deviations local circular window $\omega_\sigma(x - y)$. Moreover, $L(\psi)$ and $P(\psi)$ are the regularization and penalty terms respectively, which are defined as:

$$L(\psi) = \int |\nabla \Upsilon(\psi(x))| dx,$$

and

$$P(\psi) = \frac{1}{2} \int (|\nabla\psi(x)| - 1)^2 dx.$$

The length term is used for smoothness while the penalty term is used for re-initialization of the level set function. This model can segment images in the presence of intensity inhomogeneity and having a moderate level of noise. Increasing the noise level and inhomogeneity by the presence of backlight may lead towards weak segmentation, and this effect can be seen in figure 2. Also in images having high level of noise, the method converges very slowly. In the next section we discuss another model, which is proposed by Haider et al. [1], for handling inhomogeneity in a hybrid image data.

2.3. Double Fitting Terms of Multiplicative and Difference Images (DMD). Haider et al. [1] proposed a new segmentation model in which they used both global and local information of hybrid image. The model is based on product image as a global data term for global segmentation and the difference image is used as a local term for local segmentation. The product image is obtained by multiplying given image with its smooth version. The difference image is the difference between the filter product image and the product image. Based on this data, the following energy functional is defined as:

$$\begin{aligned} F_{DMD} &= \lambda_1 \left(\int_{in(S)} (I_0 I_0^* - a_1)^2 dx dy + \int_{out(S)} (I_0 I_0^* - a_2)^2 dx dy \right) \\ &+ \lambda_2 \left(\int_{in(S)} (\hat{w}^* - w - b_1)^2 dx dy + \int_{out(S)} (\hat{w}^* - w - b_2)^2 dx dy \right) \\ &+ \mu Length(S), \end{aligned} \quad (2.3)$$

where the average intensities for $w = I_0 I_0^*$ are a_1, a_2 and the average intensities for difference image $(\hat{w}^* - w)$ are b_1, b_2 inside and outside S . I_0^* is the filtered image of given image I_0 through convolution and \hat{w}^* is the filtered image of the product image $w = I_0 I_0^*$. This model can segment images having inhomogeneous intensity. The advantage of DMD model is that it is not sensitive to the initial contours. Also it can deal the images having inhomogeneous intensity with moderate level of noise [1]. This model is also fast in convergence. DMD model may lead to incorrect segmentation when an image has a high level of noise. Also this model could not accurately segment the desired object in images with inhomogeneous intensity and have back light effect in the background, which can be seen in figure 2. To overcome the issues of both models, we propose a novel model for segmenting images with intensity inhomogeneity and backlight effect in the background.

3. THE PROPOSED MODEL (HNI)

In this section, we have proposed a new model named as HNI for the segmentation of images having intensity inhomogeneity. The proposed model uses hybrid image data from the product of given and smooth images. To use local information we also utilized difference of product and smooth product images. Different from [1], we have used a Gaussian distribution as a fidelity term for both local and global hybrid image data. With these new data terms, we have proposed the following energy function in terms of the level

set function:

$$F_{DMD}^{LGGDF} = F_1(\cdot) + F_2(\cdot) + \nu L(\psi) + \mu P(\psi), \quad (3.4)$$

where

$$\begin{aligned} F_1(\cdot) &= \int_{in} \omega_\sigma(x-y) \left(\log(\sqrt{2\pi}) + \log(\sigma_1(x)) + \left(\frac{(u_1(x) - I_0 I_0^*)^2}{2\sigma_1(x)^2} \right) \Upsilon_1(\psi(y)) dy \right) \\ &+ \int_{out} \omega_\sigma(x-y) \left(\log(\sqrt{2\pi}) + \log(\sigma_2(x)) + \left(\frac{(u_2(x) - I_0 I_0^*)^2}{2\sigma_2(x)^2} \right) \Upsilon_2(\psi(y)) dy \right), \\ F_2(\cdot) &= \int_{in} \omega_\sigma(x-y) \left(\log(\sqrt{2\pi}) + \log(\sigma_3(x)) + \left(\frac{(u_3(x) - w - \hat{w}^*)^2}{2\sigma_3(x)^2} \right) \Upsilon_1(\psi(y)) dy \right) \\ &+ \int_{out} \omega_\sigma(x-y) \left(\log(\sqrt{2\pi}) + \log(\sigma_4(x)) + \left(\frac{(u_4(x) - w - \hat{w}^*)^2}{2\sigma_4(x)^2} \right) \Upsilon_2(\psi(y)) dy \right), \end{aligned}$$

$$L(\psi) = \int |\nabla \Upsilon(\psi(x))| dx,$$

and

$$P(\psi) = \frac{1}{2} \int (|\nabla \psi(x)| - 1)^2 dx.$$

Where the product of given image and its smooth version is denoted by $w(y) = I_0 I_0^*$ and the difference of product image and the smooth version is denoted by $\hat{w} = w - \hat{w}^*$. u_1, u_3 and σ_1, σ_3 are the local means and variances in a circular window inside the contour respectively. u_2, u_4 and σ_2, σ_4 are the local means and variances in local window outside the contour, respectively. Υ_j for $j = 1, 2$ are the characteristic functions. By keeping $\sigma_j(x)$ and ψ fixed, and minimizing equation (3.4) w.r.t. $u_j(x)$, we get:

$$\begin{aligned} u_1(x) &= \frac{\int \omega_\sigma(x-y) w(y) \Upsilon_1(\psi(y)) dy}{\int \omega_\sigma(x-y) \Upsilon_1(\psi(y)) dy} \\ u_2(x) &= \frac{\int \omega_\sigma(x-y) w(y) \Upsilon_2(\psi(y)) dy}{\int \omega_\sigma(x-y) \Upsilon_2(\psi(y)) dy} \\ u_3(x) &= \frac{\int \omega_\sigma(x-y) \hat{w}(y) \Upsilon_1(\psi(y)) dy}{\int \omega_\sigma(x-y) \Upsilon_1(\psi(y)) dy} \\ u_4(x) &= \frac{\int \omega_\sigma(x-y) \hat{w}(y) \Upsilon_2(\psi(y)) dy}{\int \omega_\sigma(x-y) \Upsilon_2(\psi(y)) dy}. \end{aligned} \quad (3.5)$$

To get optimal values of $\sigma_j(x)$, we minimize equation (3. 4) w.r.t. $\sigma_j(x)$ by keeping u_j and ψ fixed, we get:

$$\begin{aligned}\sigma_1(x)^2 &= \frac{\int \omega_\sigma(x-y)(u_1^2 - 2u_1(x)w(y) + w(y)^2)\Upsilon_1(\psi(y))dy}{\int \omega_\sigma(x-y)\Upsilon_1(\psi(y))dy} \\ \sigma_2(x)^2 &= \frac{\int \omega_\sigma(x-y)(u_2^2 + 2u_2(x)w(y) + w(y)^2)\Upsilon_2(\psi(y))dy}{\int \omega_\sigma(x-y)\Upsilon_2(\psi(y))dy} \\ \sigma_3(x)^2 &= \frac{\int \omega_\sigma(x-y)(u_3^2 - 2u_3\hat{w}(y) + \hat{w}(y)^2)\Upsilon_1(\psi(y))dy}{\int \omega_\sigma(x-y)\Upsilon_1(\psi(y))dy} \\ \sigma_4(x)^2 &= \frac{\int \omega_\sigma(x-y)(u_4^2 + 2u_4\hat{w}(y) + \hat{w}(y)^2)\Upsilon_2(\psi(y))dy}{\int \omega_\sigma(x-y)\Upsilon_2(\psi(y))dy}.\end{aligned}\quad (3. 6)$$

Now keeping $u_j(x)$ and $\sigma_j(x)$ fixed, minimizing equation (3. 4) w.r.t. ψ , the following Euler Lagrange Equation is obtained:

$$-\delta_\epsilon(\psi)(s_1 - s_2) + \nu\delta_\epsilon(\psi)\nabla \cdot \left(\frac{\nabla\psi}{|\nabla\psi|} \right) + \mu \left(\nabla^2\psi - \text{div} \left(\frac{\nabla\psi}{|\nabla\psi|} \right) \right) = 0, \quad (3. 7)$$

where s_1 and s_2 are given as:

$$\begin{aligned}s_1(x) &= \int_S \omega_\sigma(y-x) \left[\log(\sigma_1(y)) + \log(\sigma_3(y)) + \left(\frac{(u_1(x) - w(y))^2}{2\sigma_1(x)^2} \right) + \left(\frac{(u_3(x) - \hat{w}(y))^2}{2\sigma_3(x)^2} \right) \right] dy, \\ s_2(x) &= \int_S \omega_\sigma(y-x) \left[\log(\sigma_2(y)) + \log(\sigma_4(y)) + \left(\frac{(u_2(x) - w(y))^2}{2\sigma_2(x)^2} \right) + \left(\frac{(u_4(x) - \hat{w}(y))^2}{2\sigma_4(x)^2} \right) \right] dy.\end{aligned}$$

The unsteady state solution of Euler Lagrange Equation (3. 7) is

$$\frac{\partial\psi}{\partial t} = -\delta_\epsilon(\psi)(s_1 - s_2) + \nu\delta_\epsilon(\psi)\nabla \cdot \left(\frac{\nabla\psi}{|\nabla\psi|} \right) + \mu \left(\nabla^2\psi - \text{div} \left(\frac{\nabla\psi}{|\nabla\psi|} \right) \right). \quad (3. 8)$$

3.1. Algorithm of the Proposed Model (HNI).

Implementation Steps of the Proposed Method are the following:

- Step 1.** Initialize ψ as signed distance function.
- Step 2.** Find u_j , $j = 1, 2, 3, 4$ by using equation (3. 5).
- Step 3.** Update σ_j , $j = 1, 2, 3, 4$ by using equation (3. 6).
- Step 4.** Update ψ by using equation (3. 8).
- Step 5.** Return to step 2 when convergence is not achieved.

In the next section, we have discussed some of the numerical schemes used for getting the solution of partial differential equation given by equation (3. 8).

4. NUMERICAL SCHEMES

In this section we will discuss Explicit and Semi Implicit time marching schemes for the solution of equation (3. 8).

4.1. Explicit Scheme. By using explicit scheme to update ψ , equation (3. 8) can be expressed as:

$$\begin{aligned} \frac{\psi_{ij}^{n+1} - \psi_{ij}^n}{\Delta t} &= -\delta_\epsilon(\psi_{ij}^n)(s_1 - s_2) + \nu\delta_\epsilon(\psi_{ij}^n)\nabla \cdot \left(\frac{\nabla\psi_{ij}^n}{|\nabla\psi_{ij}^n|} \right) \\ &+ \mu \left(\nabla^2\psi_{ij}^n - \text{div} \left(\frac{\nabla\psi_{ij}^n}{|\nabla\psi_{ij}^n|} \right) \right), \end{aligned} \quad (4. 9)$$

it implies that:

$$\frac{\psi_{ij}^{n+1} - \psi_{ij}^n}{\Delta t} = F_{ij} + R(\psi_{ij}^n), \quad (4. 10)$$

where

$$F_{ij} = -\delta_\epsilon(\psi_{ij}^n)(s_1 - s_2),$$

and

$$R(\psi_{ij}^n) = \nu\delta_\epsilon(\psi_{ij}^n)\nabla \cdot \left(\frac{\nabla\psi_{ij}^n}{|\nabla\psi_{ij}^n|} \right) + \mu \left(\nabla^2\psi_{ij}^n - \text{div} \left(\frac{\nabla\psi_{ij}^n}{|\nabla\psi_{ij}^n|} \right) \right).$$

After arranging terms in equation (4. 10), we will get

$$\psi_{ij}^{n+1} = \psi_{ij}^n + \Delta t(F_{ij} + R(\psi_{ij}^n)). \quad (4. 11)$$

The explicit time marching scheme is conditionally stable.

4.2. Semi Implicit Scheme. Let us consider equation (3. 8) and by using semi implicit scheme we get:

$$\begin{aligned} \frac{\psi_{ij}^{n+1} - \psi_{ij}^n}{\Delta t} &= -\delta_\epsilon(\psi_{ij}^{n+1})(s_1 - s_2) + \nu\delta_\epsilon(\psi_{ij}^{n+1})\nabla \cdot \left(\frac{\nabla\psi_{ij}^{n+1}}{|\nabla\psi_{ij}^{n+1}|} \right) \\ &+ \mu \left(\nabla^2\psi_{ij}^{n+1} - \text{div} \left(\frac{\nabla\psi_{ij}^{n+1}}{|\nabla\psi_{ij}^{n+1}|} \right) \right), \end{aligned} \quad (4. 12)$$

after rearranging, we get:

$$\begin{aligned} \psi_{ij}^{n+1} &= \psi_{ij}^n - \Delta t\delta_\epsilon(\psi_{ij}^{n+1})(s_1 - s_2) + \nu\delta_\epsilon(\psi_{ij}^{n+1})\nabla \cdot \left(\frac{\nabla\psi_{ij}^{n+1}}{|\nabla\psi_{ij}^{n+1}|} \right) \\ &+ \mu \left(\nabla^2\psi_{ij}^{n+1} - \text{div} \left(\frac{\nabla\psi_{ij}^{n+1}}{|\nabla\psi_{ij}^{n+1}|} \right) \right), \end{aligned} \quad (4. 13)$$

which can be written as:

$$A(\psi^{n+1}) = F_{ij}, \quad (4. 14)$$

where A is the block tri-diagonal matrix obtained by discretization of third and fourth terms in equation (4. 13) and

$$F_{ij} = \psi_{ij}^n - \delta_\epsilon(\psi_{ij}^n)(s_1 - s_2).$$

The semi implicit scheme is unconditionally stable.

5. EXPERIMENTAL RESULTS

In this section, experimental results of the proposed model on a different gray range medical images are discussed. All experimental tests are carried out by using Matlab 2010b. Comparison of the proposed model with existing models like the LGDF and the DMD are shown in Table 1. In figure 1(a), original MR image with an initial contour is given and in figures 1(b), 1(c), 1(d), original MR image with final contour is given by using LGDF, DMD and HNI respectively. The results show that the proposed HNI model has improved the number of iterations and computational (CPU) time. In most of the experiments $\mu = 1$, $\nu = 0.001 \times 255 \times 255$, otherwise they will be mentioned. In figure 1, the performance of the proposed model is compared with the exiting LGDF and DMD models in order to detect the tumor region in a real MR image having intensity inhomogeneity. The proposed and LGDF models show similar results as shown in figures 1(b) and 1(d), but the proposed model performs better in terms of number of iterations and CPU time. Similarly the proposed model outperformed the DMD model having satisfactory results in this image.

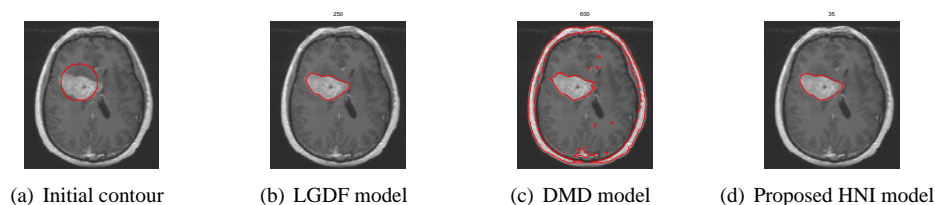


FIGURE 1. Segmentation of tumor in MR image having intensity inhomogeneity. (a) Original MR image with an initial contour (b) Original image with final contour by LGDF model (c) Original MR image with final contour by DMD model (d) Original MR image with final contour by proposed HNI model.

Figure 2 demonstrates the segmented results of a mammography image having inhomogeneous intensity achieved by the LGDF model, the DMD model and our proposed model. In figure 2, image comprises of a lesion having highlight in the whole image which causes the edges to be fuzzy. As shown in figures 2(b) and 2(c) both LGDF and DMD models are not able to segment the desirable object edges accurately specially the highlight edges of the effected part. But in figure 2(d) our proposed HNI model provides the accurate segmented result with final contour and accurately converges to the correct boundaries of all the three objects. In terms of number of iterations and CPU time our proposed HNI model performs very well as compared to other two exiting models as shown in Table 1.

The MRI of Corpus Callosum having intensity inhomogeneity is tested and segmented results with final contour are achieved by implementing the proposed model and the two existing models are shown as in figure 3. Applying the LGDF and DMD models provides the segmentation of Corpus Callosum along with the other unwanted regions in MRI as shown in figures 3(b) and 3(c). From figure 3(d) it is clear that the proposed model, in

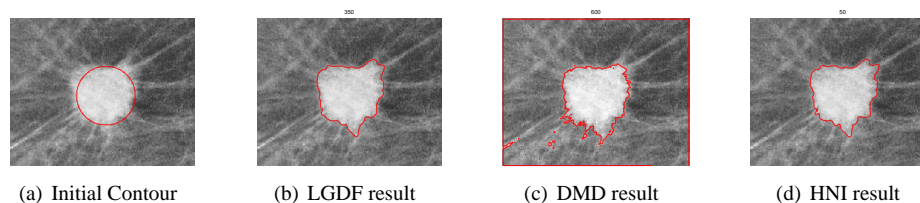


FIGURE 2. Original image with final contour. (a) Original image with Initial contour (b) LGDF result (c) DMD result (d) HNI result.

comparison to the LGDF and DMD models efficiently extracts the boundaries of the Corpus Callosum with final contour in less number of iterations and CPU time.

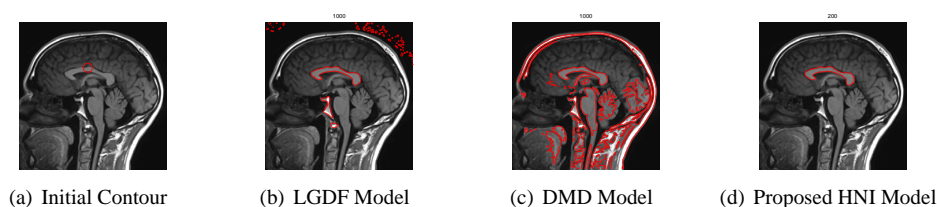


FIGURE 3. MRI image of Corpus Callosum with intensity inhomogeneity.

Figure 4 displays the comparisons of the existing models and the proposed model on medical images. Where an MRI image in the second row has been taken from the web. In figure 4(a) we can see that, both images are corrupted with intensity inhomogeneity. From figure 4(b) it is clear that the LGDF model has identified and segmented the required object accurately but it takes more iterations and CPU time. Whereas figure 4(c) shows that the DMD model has segmented the unwanted regions in addition to the desired object. Figure 4(d) shows that our proposed model has successfully segmented the desired object in both images and yields the best result in terms of iterations and CPU time as shown in Table 1. For proposed model we set $\sigma = 20$ and $\alpha = 100$ for the image in the first row of figure 4(d) and $\sigma = 7$ and $\alpha = 15$ for the image in the second row of figure 4(d).

In Table 1 and 2, problems 1, 2, 3, 4 and 5 are medical images in figures 1, 2, 3 and 4. We concluded from Table 1 that our proposed HNI model works very well and get the desirable segmented results in less number of iterations and CPU time for images having light and severe intensity inhomogeneity. Moreover, we have also used the Jaccard Similarity Index (JSI) to analyze accurately and quantitatively the truth of the desired segmented region. JSI is the ratio between the intersection and union of the segmented quantity and the ground truth quantity i.e. $JSI(M_1, M_2) = \frac{|M_1 \cap M_2|}{|M_1 \cup M_2|}$. Where M_1 is the final segmented image and M_2 is the ground truth which is obtained by manual segmentation. The value of JSI ranges from 0 to 1. When the value of JSI is closer to 1, it represents more precise segmentation. The values of JSI of segmented results are shown in Table 2.

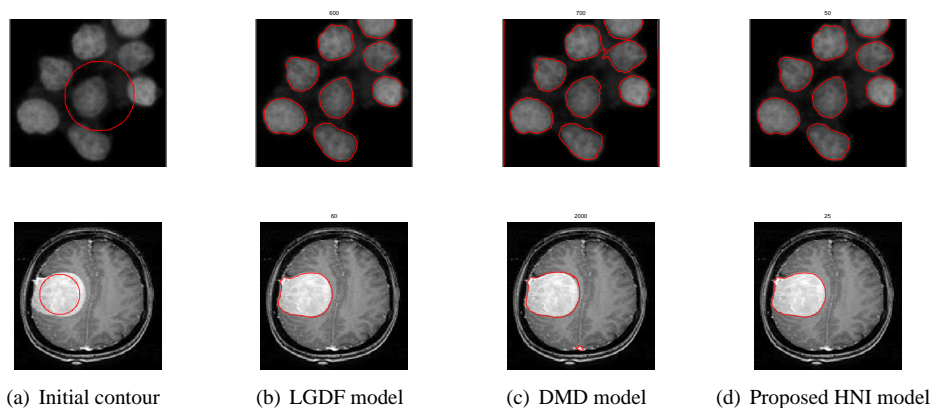


FIGURE 4. Final segmented results of cells and MRI images by (b) LGDF (c) DMD and (d) Proposed models.

TABLE 1. Comparison of LGDF and DMD models with the proposed HNI model on different images with number of iterations and CPU time.

Problems	LGDF Model		DMD Model		Proposed Model	
	Iter	CPU(sec)	Iter	CPU(sec)	Iter	CPU(sec)
1	250	7	600	116	35	4
2	350	50	600	171	50	13
3	1000	206	1000	774	200	50
4	600	120	700	137	50	10
5	60	14	2000	764	25	5

TABLE 2. Values of JSI for the segmented results of images shown in Table 1.

Models/Problems	1	2	3	4	5
LGDF	0.9755	0.6743	0.5423	0.9762	0.9882
DMD	0.2399	0.6245	0.0649	0.9373	0.8761
Proposed Model	0.999	0.997	1	0.994	0.999

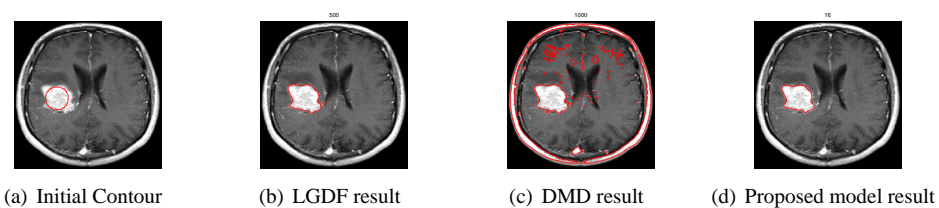


FIGURE 5. Initial Contour with segmentation results of LGDF, DMD and HNI models for brain MRI image from database.

Figure 5 shows the segmented results of MRI of the brain having tumor taken from an MRI Multiple Sclerosis Database. As shown in figure 5 the intensity in image varies throughout the tumor corresponding to the distance from the observer. Due to which it is hard to identify and segment the tumor having intensity inhomogeneity and blurred boundaries. We set the following parameters for the figure 5 as $\mu = 1$, $\nu = 0.001 \times 255 \times 255$, $\sigma = 11$ and $\alpha = 15$. From the segmented results it is clear that the proposed model effectively detects and segmented the affected region having intensity inhomogeneity in 16 seconds, whereas the LGDF and the DMD models segmented in 500 and 1000 seconds respectively and also results are not satisfactory as compared to HNI model.

Figure 6 shows the final segmented result with the contour of a brain lesion image in first row taken from the MRI MS database and digital mammography image in second row. These real medical images are corrupted with inhomogeneous intensity and also irregular with ill-defined boundaries. Because of these factors the detection and segmentation of object of interest is very hard. But the proposed model is capable to detect and segment the speculated lesion efficiently as shown in figure 6(b).

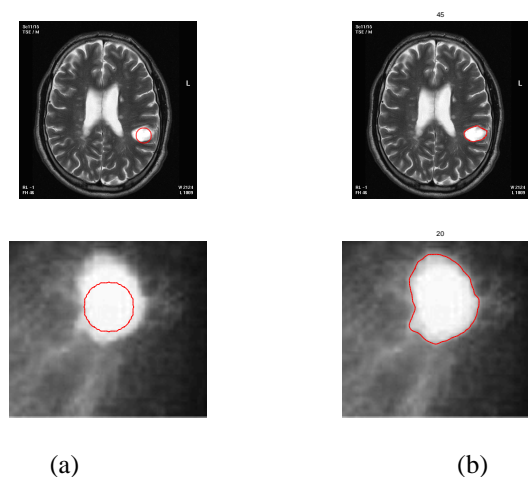


FIGURE 6. Segmented results of proposed model for medical images with inhomogeneous intensity and blurred boundaries: (a) Original image with initial contour, (b) Final segmented result of proposed model.

Figure 7 shows the final segmented outputs of the proposed model on different medical images. Experiments in figure 7 has been executed to identify the affected area in these images. Experiments demonstrate the good performance of our proposed model and shows that it works well for all medical images having inhomogeneous intensity and noise as well, as shown in figure 7. These results illustrate the capabilities of our proposed model to deal images with inhomogeneous intensity, complex background and noise.

The figure 8 demonstrates the effectiveness of the proposed HNI model in the presence of intensity inhomogeneity. All these MRI images were collected from the local hospital in Pakistan. The proposed model effectively segmented the tumors in these MRI images.

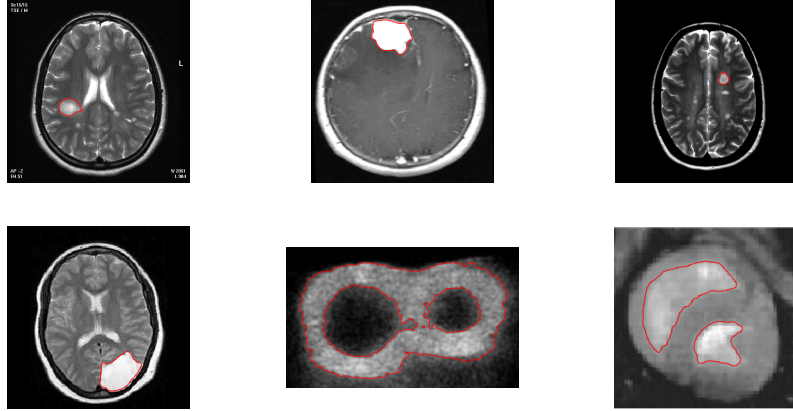


FIGURE 7. Final segmented results of different medical images by Proposed model.

In all images we have used $\mu = 0.1$ and time step = 0.1. All other parameters are indicated under the figure.

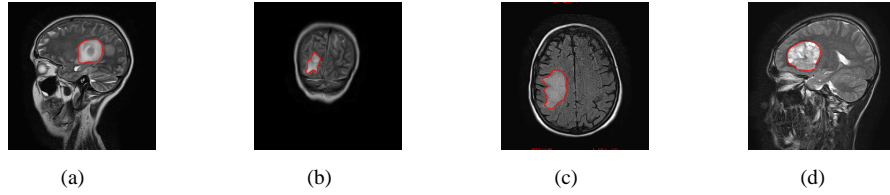


FIGURE 8. Performance of proposed HNI model in segmenting tumors in MRI images. (a) $\sigma = 22.5, \nu = 0.0025 \times 255 \times 255, \alpha = 12$; (b) $\sigma = 14, \nu = 0.001 \times 255 \times 255, \alpha = 8$; (c) $\sigma = 40, \nu = 0.001 \times 255 \times 255, \alpha = 30$; (d) $\sigma = 20, \nu = 0.0065 \times 255 \times 255, \alpha = 25$.

5.1. Parameters Sensitivity. In this section we give sensitivity of the proposed model on parameters used like σ , α and ν . We used different values of these parameters on image given in figure 1. In figure 9(a) JSI is plotted against different values of σ , where it can be seen that the best result can be obtained for $6 \leq \sigma \leq 9$ and the optimal value of σ for best segmentation result is 7. In figure 9(b) JSI is plotted against different values of α , where it can be observed that the best result can be acquired for $8.5 \leq \alpha \leq 11.5$ and the optimal value of α for best segmentation result is 10. Similarly for ν , JSI is plotted against different values of ν as shown in figure 9(c), it can be seen that the optimal value of ν of best segmentation result is $0.001 * 255 * 255$.

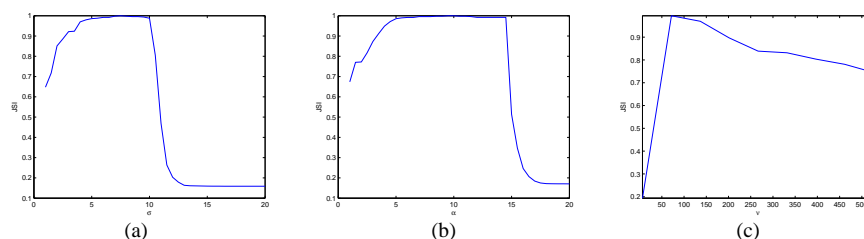


FIGURE 9. Parameters sensitivity of image in figure 1 by proposed model.

6. CONCLUSION

In order to overcome the difficulties caused by the intensity inhomogeneity and noise, we have developed a new region based variational model. The energy functional of the proposed model utilizes both the local as well as global information distribution. Our results show that the proposed model efficiently handles the images having intensity inhomogeneity and noise and therefore is able to produce a more precise image segmentation than the other existing active contour models. Furthermore, the proposed model outperforms the existing DMD and LGDF models in-terms of number of iterations and CPU time.

REFERENCES

- [1] H. Ali, N. Badshah, K. Chen and G. A. Khan, *A variational model with hybrid images data fitting energies for segmentation of images with intensity inhomogeneity*, Pattern Recognition **51**, (2016) 27–42.
- [2] R. P. Archana, *Medical application of image segmentation with intensity inhomogeneities*, International Journal of Scientific Engineering and Research **2**, (2014) 2347–3878.
- [3] T. F. Chan and L. A. Vese, *Active contours without edges*, IEEE Transaction on Image Processing **10**, (2001) 266–277.
- [4] J. Duan, Z. Pan, X. Yin, W. Wei and G. Wang, *Some fast projection methods based on Chan-Vese model for image segmentation*, EURASIP Journal on Image and Video Processing **7**, (2014) 1–16.
- [5] S. Fishan, L. Mabood, H. Ali and N. Badshah, *Active contour model based on local signed pressure force functions*, Punjab University Journal of Mathematics **51**, No. 4 (2019) 113–129.
- [6] C. Huang and L. Zeng, *An active contour model for the segmentation of images with intensity inhomogeneities and bias field estimation*, PLOS ONE **10**, (2015) 1–24.
- [7] M. Kass, A. Witkin and D. Terzopoulos, *Snakes: active contour models*, International Journal of Computer Vision **4**, (1987) 321–331.
- [8] C. Li, R. Huang, Z. Ding, J. C. Gatenby, D. N. Metaxas and J. C. Gore, *A level set method for image segmentation in the presence of intensity inhomogeneities with application to MRI*, IEEE Transaction on Image Processing **20**, (2011) 2007–2016.
- [9] S. Liu, Y. Peng, G. Qiu and X. Hao, *A locally statistical active contour model for image segmentation with intensity inhomogeneity*, International Journal of Mobile Computing and Multimedia Communications **6**, (2014) 33–49.
- [10] S. Liu and Y. Peng, *A local region-based Chan-Vese model for image segmentation*, Pattern Recognition **45**, (2012) 2769–2779.
- [11] C. Li, C. Kao, J. Gore and Z. Ding, *Implicit active contours driven by local binary fitting energy*, 2007 IEEE Conference on Computer Vision and Pattern Recognition, (2007) 1–7.
- [12] D. Mumford and J. Shah, *Optimal approximations by piecewise smooth functions and associated variational problems*, Communication on Pure and Applied Mathematics **42**, No. 5 (1989) 557–685.
- [13] Y. Peng, F. Liu and S. Liu, *A normalized local binary fitting model for image segmentation*, Fourth International Conference on Intelligent Networking and Collaborative Systems, (2012) 77–80.

- [14] L. Wang, L. He, A. Mishra and C. Li, *Active contours driven by local gaussian distribution fitting energy*, *Signal Processing* **89**, (2009) 2435–2447.
- [15] L. Wang, Y. Chen, X. Pan, X. Hong and D. Xia, *Level set segmentation of brain magnetic resonance images based on local gaussian distribution fitting energy*, *Journal of Neuroscience Methods* **188**, (2010) 316–325.
- [16] L. Wang, H. Zhang, K. He, Y. Chang and X. Yanget, *Active contours driven by multi-feature gaussian distribution fitting energy with application to vessel segmentation*, *PLOS ONE* **10**, (2015) 1–8.
- [17] Y. Yunyun and W. Boying, *Convex image segmentation model based on local and global intensity fitting energy and split bregman method*, *Journal of Applied Mathematics*, (2012) 1–16.
- [18] K. Zhang, L. Zhang, K. Lam and D. Zhang, *A level set approach to image segmentation with intensity inhomogeneity*, *IEEE Transaction on Cybernetics* **46**, (2016) 546–557.
- [19] N. Zhang, J. Zhang and R. Shi, *An improved Chan-Vese model for medical image segmentation*, 2008 International Conference on Computer Science and Software Engineering, (2008), doi: 10.1109/CSSE.2008.826.